Cortical Representations of Speech in a Multi-talker Auditory Scene

Krishna C. Puvvada[a], Jonathan Z. Simon[a,b,c]

[a] Department of Electrical & Computer Engineering, University of Maryland, College Park, MD 20742

[b] Department of Biology, University of Maryland, College Park, MD 20742

[c] Institute for Systems Research, University of Maryland, College Park, MD 20742

Corresponding author: Jonathan Z. Simon (jzsimon@umd.edu), Department of Electrical & Computer Engineering, University of Maryland, 8223 Paint Branch Dr., College Park, MD 20742.

Abbreviated title: **Foreground and Background Speech Representations**

Number of pages: 43

Number of figures: 5

Number of words in Abstract: 211

Number of words in Introduction: 649

Number of words in Discussion: 1493

Conflict of Interest: The authors declare no competing financial interests.

Acknowledgements: The authors thank Elizabeth Nguyen for excellent MEG technical support, and Stuart Rosen for advice on the stimulus paradigm. This work was supported by NIH grant R01 DC014085.

Abstract

The ability to parse a complex auditory scene into perceptual objects is facilitated by a hierarchical auditory system. Successive stages in the hierarchy transform an auditory scene of multiple overlapping sources, from peripheral tonotopically-based representations in the auditory nerve, into perceptually distinct auditory-objects based representation in auditory cortex. Here, using magnetoencephalography (MEG) recordings from human subjects, we investigate how a complex acoustic scene consisting of multiple speech sources is represented in distinct hierarchical stages of auditory cortex. Using systems-theoretic methods of stimulus reconstruction, we show that the primary-like areas in auditory cortex contain dominantly spectro-temporal based representations of the entire auditory scene. Here, both attended and ignored speech streams are represented with almost equal fidelity, and a global representation of the full auditory scene with all its streams is a better candidate neural representation than that of individual streams being represented separately. In contrast, we also show that higher order auditory cortical areas represent the attended stream separately, and with significantly higher fidelity, than unattended streams. Furthermore, the unattended background streams are more faithfully represented as a single unsegregated background object rather than as separated objects. Taken together, these findings demonstrate the progression of the representations and processing of a complex acoustic scene up through the hierarchy of human auditory cortex.

43 **Significance Statement:**

44 Using magnetoencephalography (MEG) recordings from human listeners in a
45 simulated cocktail party environment, we investigate how a complex acoustic
46 scene consisting of multiple speech sources is represented in separate hierarchical
47 stages of auditory cortex. We show that the primary-like areas in auditory cortex
48 use a dominantly spectro-temporal based representation of the entire auditory
49 scene, with both attended and ignored speech streams represented with almost
50 equal fidelity. In contrast, we show that higher order auditory cortical areas
51 represent an attended speech stream separately from, and with significantly higher
52 fidelity than, unattended speech streams. Furthermore, the unattended background
53 streams are represented as a single undivided background object rather than as
54 distinct background objects.
55

Introduction

Individual sounds originating from multiple sources in a complex auditory scene mix linearly and irreversibly before they enter the ear, yet are perceived as distinct objects by the listener (Cherry, 1953; Bregman, 1994; McDermott, 2009). The separation, or rather individual re-creation, of such linearly mixed original sound sources is a mathematically ill-posed question, yet the brain nevertheless routinely performs this task with ease. The neural mechanisms by which this perceptual 'un-mixing' of sounds occur, the collective cortical representations of the auditory scene and its constituents, and the role of attention in both, are key problems in contemporary auditory neuroscience.

It is known that auditory processing in primate cortex is hierarchical (Davis and Johnsrude, 2003; Hickok and Poeppel, 2007; Rauschecker and Scott, 2009; Okada et al., 2010; Peelle et al., 2010; Overath et al., 2015) with subcortical areas projecting onto the core areas of auditory cortex, and from there, on to belt, parabelt and additional auditory areas (Kaas and Hackett, 2000). Sound entering the ear reaches different anatomical/functional areas of auditory cortex with different latencies (Recanzone et al., 2000; Nourski et al., 2014). Due to this serial component of auditory processing, the hierarchy of processing can be described by both anatomy and latency, of which the latter may be exploited using the high

temporal fidelity of non-invasive magnetoencephalography (MEG) neural recordings.

In selective listening experiments using natural speech and MEG, the two major neural responses known to track the speech envelope are the $M50_{TRF}$ and $M100_{TRF}$, with respective latencies of 30 – 80 ms and 80 – 150 ms, of which the dominant neural sources are, respectively, Heschl's gyrus (HG) and Planum temporale (PT) (Steinschneider et al., 2011; Ding and Simon, 2012b). Posteromedial HG is the site of core auditory cortex; PT contains both belt and parabelt auditory areas (here collectively referred to as higher-order areas) (Griffiths and Warren, 2002; Sweet et al., 2005). Hence the earlier neural responses are dominated by core auditory cortex, and the later are dominated by higher-order areas. To better understand the neural mechanisms of auditory scene analysis, it is essential to understand how the cortical representations of a complex auditory scene change from the core to the higher order auditory areas.

One topic of interest is whether the brain maintains distinct neural representations for each unattended source (in addition to the representation of the attended source), or if all unattended sources are represented collectively as a single monolithic background object. A common paradigm used to investigate the neural mechanisms underlying auditory scene analysis employs a pair of speech streams, of which one is attended, which then leaves the other speech stream

remaining as the background (Kerlin et al., 2010; Ding and Simon, 2012b; Mesgarani and Chang, 2012; Power et al., 2012; Zion Golumbic et al., 2013b; O'Sullivan et al., 2015). This results in a limitation, which cannot address the question of distinct vs. collective neural representations for unattended sources. This touches on the long-standing debate of whether auditory object segregation is pre-attentive or it is actively influenced by attention (Carlyon, 2004; Sussman et al., 2005; Shinn-Cunningham, 2008; Shamma et al., 2011). Evidence for segregated neural representations of background streams would support the former, whereas a lack of segregated background objects would support the latter.

To address these issues, we use MEG to investigate a variety of potential cortical representations of the elements of a multi-talker auditory scene. We test two major hypotheses: that the dominant representation in core auditory cortex is of the physical acoustics, not of separated auditory objects; and that once object-based representations emerge in higher order auditory areas, the unattended contributions to the auditory scene are represented collectively as a single background object. The methodological approach employs the linear systems methods of stimulus prediction and MEG response reconstruction (Lalor et al., 2009; Mesgarani et al., 2009; Ding and Simon, 2012b; Mesgarani and Chang, 2012; Pasley et al., 2012; Di Liberto et al., 2015).

Materials & Methods:

Subjects & Experimental Design Nine normal-hearing, young adults (6 Female) participated in the experiment. All subjects were paid for their participation. The experimental procedures were approved by the University of Maryland Institutional Review Board. Subjects listened to a mixture of three speech segments spoken by, respectively, a male adult, female adult and a child speaker. The three speech segments were mixed into a single audio channel with equal perceptual loudness. All three speech segments were taken from public domain narration of Grimms' Fairy Tales by Jacob & Wilhelm Grimm (https://librivox.org/fairy-tales-by-the-brothers-grimm/). Periods of silence longer than 300 ms were replaced by a shorter gap whose duration was chosen randomly between 200 ms and 300 ms. The audio signal was low-pass filtered below 4 kHz. In first of three conditions, the subjects were asked to attend to the child speaker, while ignoring the other two (i.e., child speaker as target, with male and female adult speakers as background). In condition two, during which the same mixture was played as in condition one, the subjects were instead asked to attend to the male adult speaker (with female adult and child speakers as background). Similarly, in condition three, the target was switched to the female adult speaker. Each condition was repeated three times successively, producing three trials per condition. The presentation order of the three conditions was counterbalanced

across subjects. Each trial was of 220 s duration, divided into two 110 s sections, to reduce listener fatigue. To help participants attend to the correct speaker, the first 30 s of each section was replaced by the clean recording of the target speaker alone, followed by a 5 s upward linear ramp of the background speakers. Recordings of this first 35 s of each segment were not included in any analysis. To further encourage the subjects to attend to the correct speaker, a target-word was set before each trial and the subjects were asked to count the number of occurrences of the target-word in the speech of the attended speaker. Additionally, after each condition, the subject was asked to recount a short summary of the attended narrative. The subjects were required to close their eyes while listening. Before the main experiment, 100 repetitions of a 500-Hz tone pip were presented to each subject to elicit the M100 response, a reliable auditory response occurring ~100 ms after the onset of a tone pip. This data was used check whether any potential subjects gave abnormal auditory responses, but no subjects were excluded based on this criterion.

Data recording and pre-processing MEG recordings were conducted using a 160-channel whole-head system (Kanazawa Institute of Technology, Kanazawa, Japan). Its detection coils are arranged in a uniform array on a helmet-shaped surface of the bottom of the dewar, with ~25 mm between the centers of two

adjacent 15.5-mm-diameter coils. Sensors are configured as first-order axial gradiometers with a baseline of 50 mm; their field sensitivities are 5 fT/$\sqrt{}$Hz or better in the white noise region. Subjects lay horizontally in a dimly lit magnetically shielded room (Yokogawa Electric Corporation). Responses were recorded with a sampling rate of 1 kHz with an online 200-Hz low-pass filter and 60 Hz notch filter. Three reference magnetic sensors and three vibrational sensors were used to measure the environmental magnetic field and vibrations. The reference sensor recordings were utilized to reduce environmental noise from the MEG recordings using the Time-Shift PCA method (de Cheveigne and Simon, 2007). Additionally, MEG recordings were decomposed into virtual sensors/ components using denoising source separation (DSS) (Särelä and Valpola, 2005; de Cheveigne and Simon, 2008; de Cheveigne and Parra, 2014), a blind source separation method that enhances neural activity consistent over trials. Specifically, DSS decomposes the multichannel MEG recording into temporally uncorrelated components, where each component is determined by maximizing its trial-to-trial reliability, measured by the correlation between the responses to the same stimulus in different trials. To reduce the computational complexity, for all further analysis the 157 MEG sensors were reduced, using DSS, to 4 components in each hemisphere. Also, both stimulus envelope and MEG responses were band pass

174 filtered between 1 – 8 Hz (delta and theta bands), which correspond to the slow
175 temporal modulations in speech (Ding and Simon, 2012a, b).
176
177 ***Terminology and Notation*** As specified in the stimulus description, in each
178 condition the subject attends to one among the three speech streams. The envelope
179 of attended speech stream is referred to as the 'foreground' and the envelope of
180 each of the two unattended speech streams is referred to as the 'individual
181 background'. In contrast, the envelope of the entire unattended part of the
182 stimulus, comprising *both* unattended speech streams, is referred to as the
183 'combined background'. The envelope of entire acoustic stimulus or auditory
184 scene, comprising of all the three speech streams is referred to as the 'acoustic
185 scene'. Thus, if S_a, S_b, S_c are three speech stimuli, $Env(S_a + S_b + S_c)$ is the
186 acoustic scene. In contrast, the sum of envelopes of three speech streams,
187 $Env(S_a) + Env(S_b) + Env(S_c)$, is referred to as the 'sum of streams', and the
188 two are not mathematically equal: even though both are functions of the same
189 stimuli, they differ due to the non-linear nature of a signal envelope (the linear
190 correlation between the acoustic scene and the sum of streams is typically ~0.75).
191 Neural responses with latencies less than ~85 ms (typically originating
192 from core auditory areas) are referred to here as 'early neural responses' and
193 responses with latencies more than ~85 ms (typically from higher-order auditory

194 areas) (Ahveninen et al., 2011; Okamoto et al., 2011; Steinschneider et al., 2011)
195 are referred to as 'late neural responses'.
196
197 ***Temporal Response Function*** In an auditory scene with a single talker, the
198 relation between MEG neural response and the presented speech stimuli can be
199 modeled using a linear temporal response function (TRF) as

$$r(t) = \sum_{\tau} s(t-\tau)TRF(\tau) + \varepsilon(t) \quad (1)$$

200 where $t = 0,1, \ldots, T$ is time, $r(t)$ is the response from any individual sensor or
201 DSS component, $s(t)$ is the stimulus envelope in decibels, $TRF(t)$ is the TRF
202 itself, and $\epsilon(t)$ is residual response waveform not explained by the TRF model
203 (Ding and Simon, 2012a). The envelope is extracted by averaging the auditory
204 spectrogram, (Chi et al., 2005) along the spectral dimension. The TRF is estimated
205 using boosting with 10-fold cross-validation (David et al., 2007). In case of single
206 speech stimuli, the TRF is typically characterized by a positive peak between 30
207 ms and 80 ms and a negative peak between 90 ms and 130 ms, referred to as
208 $M50_{TRF}$ and $M100_{TRF}$ respectively (Ding and Simon, 2012b) (positivity/negativity
209 of the magnetic field is by convention defined to agree with the corresponding
210 electroencephalography[EEG] peaks). Success/accuracy of the linear model is
211 evaluated by how well it predicts neural responses, as measured by the proportion

of the variance explained: the square of the Pearson correlation coefficient between the MEG measurement and the TRF model prediction.

In the case of more than one speaker, the MEG neural response, $r(t)$ can be modeled as the sum of the responses to the individual acoustic sources (Ding and Simon, 2012b; Zion Golumbic et al., 2013b), referred to here as the 'Summation model'. For example, with two speech streams, the neural response would be modeled as

$$r(t) = \sum_{\tau} S_a(t-\tau)TRF_a(\tau) + \sum_{\tau} S_b(t-\tau)TRF_b(\tau) + \varepsilon(t) \qquad (2)$$

where $S_a(t)$ and $S_b(t)$ are the envelopes of the two speech streams, and $TRF_a(t)$, and $TRF_b(t)$ are the TRFs corresponding to each stream. The summation model is easily extended to the case of more than two speech streams, by adding new terms with each new individual speech stream envelope and the corresponding TRF.

In addition to the existing summation model, we propose a new encoding-model referred to as the 'Early-late model', which allows one to incorporate the hypothesis that the early neural responses typically represent the entire acoustic scene, but that the later neural responses differentially represent the separated foreground and background.

$$r(t) = \sum_{\tau=0}^{\tau=\tau_1} S_A(t-\tau)TRF_A(\tau) + \sum_{\tau=\tau_1}^{\tau=\tau_2} S_F(t-\tau)TRF_F(\tau) + \sum_{\tau=\tau_1}^{\tau=\tau_2} S_B(t-\tau)TRF_B(\tau) + \epsilon(t) \qquad (3)$$

where $S_A(t)$ is the (entire) acoustic scene, $S_F(t)$ is the envelope of attended (foreground) speech stream, and $S_B(t)$ is the combined background (i.e., envelope of everything other than attended speech stream in the auditory scene), and $TRF_A(t), TRF_F(t),$ and $TRF_B(t)$ are the corresponding $TRFs. \tau_1, \tau_2$ represent the boundary values of the integration windows for early and late neural responses respectively.

The explanatory power of different models, such as the Summation and Early-late models, can be ranked by comparing the accuracy of their response predictions (illustrated in Figure 1, left).

(Figure 1 about here)

Decoding speech from neural responses While the TRF/encoding analysis described in the previous section predicts neural response from the stimulus, decoding analysis reconstructs the stimulus based on the neural response. Thus, decoding analysis complements the TRF analysis (Mesgarani et al., 2009). Mathematically the envelope reconstruction/decoding operation can be formulated as

$$E(t) = \sum_{k=1}^{N} \sum_{\tau=\tau_b}^{\tau_e} M_k(t+\tau) D_k(\tau) + \epsilon(t) \quad (4)$$

where $E(t)$ is the reconstructed envelope, $M_k(t)$ is the MEG recording (neural response) from sensor/component k, and $D_k(t)$ is the linear decoder for sensor/component k. The times τ_b and τ_e denote the beginning and end times of the integration window. By appropriately choosing the values of τ_b and τ_e, envelope reconstructions using neural responses from any desired time window can be compared. The decoder is estimated using boosting analogously to the TRF estimation in the previous section. In the single talker case the envelope is of that talker's speech. In a multi-talker case, the envelope to be reconstructed might be the envelope of the speech of attended talker, or one of the background talkers, or of a mixture of any two or all three talkers, depending on the model under consideration. Chance-level reconstruction (i.e., the noise floor) from a particular neural response is estimated by reconstructing an unrelated stimulus envelope from that neural response. Figure 2 illustrates the distinction between reconstruction of stimulus envelope from early and late responses. The stimulus envelope at time point *t* can be reconstructed using neural responses from the dashed (early response) window or dotted (late response) window. (While it is true that the late responses to the stimulus at time point $t - \Delta t$ overlap with early responses to the stimulus at time point *t*, the decoder used to reconstruct the stimulus at time point *t* from early responses is only minimally affected by late responses to the stimulus at time point $t - \Delta t$ when the decoder is estimated by

averaging over a long enough duration, e.g., tens of seconds). The cut-off time between early and late responses, $\tau_{boundary}$, was chosen to minimize the overlap between the $M50_{TRF}$ and $M100_{TRF}$ peaks, on a per subject basis, with a typical value being 85 ms. When decoding from early responses only, the time window of integration is from $\tau_b = 0$ to $\tau_e = \tau_{boundary}$. When decoding from late neural responses only, the time window of integration is from $\tau_b = \tau_{boundary}$ to $\tau_e =$ 500 ms.

(Figure 2 about here)

The robustness of different representations, such as of Foreground vs. Background, can be compared by examining the accuracy of their respective stimulus envelope reconstructions (illustrated in Figure 1, right).

Statistics All statistical comparisons reported here are two-tailed permutation tests with N=1,000,000 random permutations (within subject). Due to the value of N selected, the smallest accurate p value that can be reported is $2\times1/N$ ($= 2\times10^{-6}$; the factor of 2 arises from the two-tailed test) and any p value smaller than $2/N$ is reported as $p < 2\times10^{-6}$. The statistical comparison between foreground and individual backgrounds requires special mention, since each listening condition

has one foreground but two individual backgrounds. From the perspective of both behavior and task, both the individual backgrounds are interchangeable. Hence, when comparing reconstruction accuracy of foreground vs. individual background the average reconstruction accuracy of the two individual backgrounds is used. Finally, Bayes factor analysis is used, when appropriate, to evaluate evidence in favor of null hypothesis, since conventional hypothesis testing is not suitable for such purposes. Briefly, Bayes factor analysis calculates the *posterior odds* i.e., the ratio of $P(H_0|observations)$ to $P(H_1|observations)$, where H_0 and H_1 are the null and alternate hypotheses respectively.

$$\frac{P(H_0|observations)}{P(H_1|observations)} = \frac{P(observations|H_0)}{P(observations|H_1)} \times \frac{P(H_0)}{P(H_1)} \quad (5)$$

$$= BF_{01} \times \frac{P(H_0)}{P(H_1)} \quad (6)$$

The ratio of $P(observations|H_0)$ and $P(observations|H_1)$ is denoted as the Bayes factor, BF_{01}. Then, under the assumption of equal priors ($P(H_0) = P(H_1)$), the posterior odds reduces to BF_{01}. A BF_{01} value of 10 indicates that the data is ten times more likely to occur under the null hypothesis than the alternate hypothesis; conversely, a BF_{01} value of 0.1 indicates that the data is 10 times more likely to occur under the alternate hypothesis than the null hypothesis. Conventionally, a BF_{01} value between 3 and 10 is considered as moderate evidence in favor of the

null hypothesis, and a value between 10 and 30 is considered strong evidence; conversely, a BF_{01} value between 1/3 & 1/10 (respectively 1/10 & 1/30) is considered moderate (respectively strong) evidence for the alternate hypothesis (for more details we refer the reader to Rouder et al. (2009)).

Results

Stimulus reconstruction from early neural responses

To investigate the neural representations of the attended vs. unattended speech streams associated with early auditory areas, i.e., from core auditory cortex, (Nourski et al., 2014), the temporal envelope of attended (foreground) and unattended speech streams (individual backgrounds) were reconstructed using decoders optimized individually for each speech stream. All reconstructions performed significantly better than chance level (foreground vs. noise, $p < 2\times10^{-6}$; individual background vs. noise, $p < 2\times10^{-6}$), indicating that all three speech streams are represented in early auditory cortex. Figure 3A shows reconstruction accuracy for foreground vs. individual backgrounds. A permutation test shows no significant difference between foreground and individual background ($p = 0.21$), indicating that there is no evidence of significant neural bias for the attended speech stream over the ignored speech stream, in early neural responses. In fact, Bayes Factor analysis ($BF_{01} = 4.2$) indicates moderate support in favor of the null

hypothesis (Rouder et al., 2009), that early neural responses do not distinguish significantly between attended and ignored speech streams.

(Figure 3 about here)

To test the hypothesis that early auditory areas represent the auditory scene in terms of acoustics, rather than as individual auditory objects, we reconstructed the acoustic scene (the envelope of the sum of all three speech streams) and compared it against the reconstruction of the sum of streams (sum of reconstruction envelopes of each of the three individual speech streams). Separate decoders optimized individually were used to reconstruct the acoustic scene and the sum of streams. As can be seen in Figure 3B, the result shows that the acoustic scene is better reconstructed than the sum of streams ($p < 2\times10^{-6}$). This indicates that early auditory cortex is better described as processing the entire acoustic scene rather than processing the separate elements of the scene individually.

Stimulus reconstruction from late neural responses

While the preceding results were based on early cortical processing, the following results are based on late auditory cortical processing (responses with latencies more than ~85 ms). Figure 4A shows the scatter plot of reconstruction accuracy

for the foreground vs. individual background envelopes based on late responses. A paired permutation test shows that reconstruction accuracy for the foreground is significantly higher than the background ($p < 2\times10^{-6}$). Even though the individual backgrounds are not as reliably reconstructed as foreground, their reconstructions are nonetheless significantly better than chance level ($p < 2\times10^{-6}$).

In order to distinguish among possible neural representations of the background streams, we compared the reconstructability of the envelope of the entire background as a whole, with the reconstructability of the sum of the envelopes of the (two) backgrounds. If the background is represented as a single auditory object (i.e., "the background"), the reconstruction of the envelope of the entire background should be more faithful than the sum of envelopes of individual backgrounds. In contrast, if the background is represented as distinct auditory objects, each distinguished by its own envelope, the reconstruction of the sum of envelopes of the individual backgrounds should be more faithful. Figure 4B shows the scatter plot of reconstruction accuracy for the envelope of combined background vs. the sum of the envelopes of the individual background streams. Analysis shows that the envelope of the combined background is significantly better represented than the sum of the individual envelopes of the individual backgrounds ($p = 0.012$). As noted previously, the envelope of the combined background is actually strongly correlated with the sum of the envelopes of the

individual backgrounds, meaning that finding a significant difference in their reconstruction accuracy is *a priori* unlikely, providing even more credence to the result.

(Figure 4 about here)

Encoding analysis

Results above from envelope reconstruction suggest that while early neural responses represent the auditory scene in terms of the acoustics, the later neural responses represent the auditory scene in terms of a separated foreground and a single background stream. In order to further test this hypothesis, we use TRF-based encoding analysis to directly compare two different models of auditory scene representations. The two models compared are the standard Summation model (based on parallel representations of all speech streams; see Equation 2) and the new Early-late model (based on an early representation of the entire acoustic scene and late representations of separated foreground and background; see Equation 3). Figure 5 shows the response prediction accuracies for the two models. A permutation test shows that the accuracy of the Early-late model is considerably higher than that of the Summation model ($p < 2\times10^{-6}$). This indicates that a model in which early/core auditory cortex processes the entire acoustic

scene but later/higher-order auditory cortex processes the foreground and background separately has more support than the previously employed model of parallel processing of separate streams throughout auditory cortex.

(Figure 5 about here)

Discussion

In this study, we used cortical tracking of continuous speech, in a multi-talker scenario, to investigate the neural representations of an auditory scene. Differing latencies of the neural sources processing the same stimuli allow us to separate the source activity temporally, thus enabling the tracking of differing neural representations of the auditory scene. From MEG recordings of subjects selectively attending to one of the three co-located speech streams, we observed that 1) The early neural responses (with short latencies), which originate primarily from core auditory cortex, represent the foreground (attended) and background (ignored) speech streams without any significant difference, whereas the late neural responses (with longer latencies), which originate primarily from higher-order areas of auditory cortex, represent the foreground with significantly higher fidelity than the background; 2) Early neural responses are not only balanced in how they represent the constituent speech streams, but in fact represent the entire

404 acoustic scene holistically, rather than as separately contributing individual
405 perceptual objects; 3) Even though there are two physical speech streams in the
406 background, no neural segregation is observed for the background speech streams.
407 It is well established that auditory processing in cortex is performed in a
408 hierarchical fashion, in which an auditory stimulus is processed by different
409 anatomical areas at different latencies (Inui et al., 2006; Nourski et al., 2014).
410 Using this idea to inform the neural decoding/encoding analysis allows the
411 effective isolation of neural signals from a particular cortical area, and thereby the
412 ability to track changes in neural representations as the stimulus processing
413 proceeds along the auditory hierarchy. This time-constrained
414 reconstruction/prediction approach may prove especially fruitful in high-time-
415 resolution/low-spatial-resolution imaging techniques such as MEG and EEG. Even
416 though different response components are generated by different neural sources,
417 standard neural source localization algorithms may perform poorly when different
418 sources are strongly correlated in their responses (Lutkenhoner and Mosher,
419 2007). While the proposed method is not to be viewed as an alternative to source
420 localization methods, it can nonetheless be used to tease apart different
421 components of MEG/EEG response, without explicit source localization.
422 The envelope reconstruction using the early, auditory core, neural response
423 component showed no significant difference between foreground and background,

in contrast to reconstruction using the late, higher-order auditory, neural responses, where the foreground is substantially better represented than any individual background. This *decoding* result is in agreement with the *encoding* result of (Ding and Simon, 2012b) where the authors showed that the early $M50_{TRF}$ component of the temporal response function is not significantly modulated by attention, whereas the late $M100_{TRF}$ component is modulated by attention.

Even though there is no significant difference between the ability to reconstruct the foreground and background from early neural responses, nonetheless we observe a non-significant tendency towards an enhanced representation of the foreground (foreground > background, $p = 0.21$). This could be due to task-related plasticity of spectro-temporal receptive fields of neurons in mammalian primary auditory cortex (Fritz et al., 2003), where the receptive fields of neurons are tuned to match the stimulus characteristics of attended sounds. It could also be explained by entrainment (Schroeder and Lakatos, 2009; Zion Golumbic et al., 2012), which postulates that the high excitability periods of neurons become aligned with temporal structure of foreground, thereby enhancing its neural representation.

The increase in fidelity of the foreground as the response latency increases, from early neural responses (from core auditory cortex) to late neural responses

(from higher-order auditory cortex), indicates a temporal as well as functional hierarchy in cortical processing of auditory scene, from core to higher-order areas in auditory cortex. Similar preferential representation for the attended speech stream has been demonstrated, albeit with only two speech streams, using delta and theta band neural responses (Ding and Simon, 2012b; Zion Golumbic et al., 2013a; Zion Golumbic et al., 2013b) as well as high-gamma neural responses (Mesgarani and Chang, 2012; Zion Golumbic et al., 2013a), and using monaural (Ding and Simon, 2012b; Mesgarani and Chang, 2012) as well as audio-visual speech (Zion Golumbic et al., 2013a; Zion Golumbic et al., 2013b).

While some researchers suggest a selective entrainment model (Schroeder and Lakatos, 2009; Ng et al., 2012; Zion Golumbic et al., 2013b; Kayser et al., 2015) as the mechanism underlying the selective tracking of attended speech, others suggest a temporal coherence model (Shamma et al., 2011; Ding and Simon, 2012b) as the neuronal mechanism underlying selective tracking. Natural speech is quasi-rhythmic with different dominant rates at syllabic, word and prosodic frequencies. The selective entrainment model suggests that attention causes endogenous low frequency neural oscillations to align with the temporal structure of the attended speech stream, thus aligning the high excitability phases of oscillations with events in attended stream. This effectively forms a mask that favors the attended speech. The temporal coherence model suggests that selective

464 tracking of attended speech is achieved through two stages. First is a cortical
465 filtering stage, where feature selective neurons filter the stimulus producing a
466 multidimensional representation of auditory scene along different feature axes.
467 This is followed by a second stage, coherence analysis, which combines different
468 features streams based on their temporal similarity, giving rise to separate
469 perceptions of attended and ignored streams.

470 The representation of an auditory scene in core auditory cortex is here
471 shown to be more spectro-temporal- or acoustic-based than object-based, as
472 demonstrated by the result that the envelope of the auditory scene is better
473 reconstructed than the sum of envelopes of the individual speech streams (e.g.,
474 Figure 3B). This is further supported by the result that the Early-late model
475 predicts MEG neural responses significantly better than Summation model (e.g.,
476 Figure 5). This is consistent with previous studies that demonstrated that neural
477 activity in core auditory cortex was highly sensitive to acoustic characteristics of
478 speech and primarily reflects spectro-temporal attributes of sound (Nourski et al.,
479 2009; Okada et al., 2010; Steinschneider et al., 2014). All these results suggest that
480 early neural responses, primarily from core auditory cortex, reflect an acoustic-
481 based representation rather than object-based. In contrast, Nelken and Bar-Yosef
482 (2008) suggest that neural auditory objects may form as early as primary auditory
483 cortex, and Fritz et al. (2003) show that representations of dynamic sounds in

484 primary auditory cortex are influence by task. It is possible that less complex
485 stimuli are resolved earlier in the hierarchy of auditory pathway (e.g., sounds that
486 can be separated via tonotopy) whereas speech streams, which overlap both
487 spectrally and temporally, are resolved only much later in auditory pathway.

488 It is widely accepted that an auditory scene is *perceived* in terms of
489 auditory objects (Bregman, 1994; Griffiths and Warren, 2004; Shinn-Cunningham,
490 2008; Shamma et al., 2011). Ding and Simon (2012a) demonstrated evidence for
491 an object-based cortical representation of an auditory scene, but did not distinguish
492 between early and late neural responses. This, coupled with the result here that
493 early neural responses provide an acoustic, not object-based, representation,
494 strongly suggest that the object-based representation emerges only in the late
495 neural responses/higher-order (belt and parabelt) auditory areas. This is further
496 supported by the observation that acoustic invariance, a property of object-based
497 representation, is observed in higher order areas but not in core auditory cortex
498 (Chang et al., 2010; Okada et al., 2010).

499 When the foreground is represented as an auditory object in late neural
500 responses, the finding that the combined background is better reconstructed than
501 the sum of envelopes of individual backgrounds (Figure 4B) suggests that in late
502 neural responses the background is not represented as separated and distinct
503 auditory objects. This result is consistent with that of Sussman et al. (2005), who

reported an unsegregated background when subjects attended to one of three tone streams in the auditory scene. This unsegregated background may be a result of an 'analysis-by-synthesis' (Yuille and Kersten, 2006; Poeppel et al., 2008) mechanism, wherein the auditory scene is first decomposed into basic acoustic elements, followed by top-down processes that guide the synthesis of the relevant components into a single stream, which then becomes the object of attention. The remainder of the auditory scene would be the unsegregated background, which itself might have the properties of an auditory object. When attention shifts, new auditory objects are correspondingly formed, with the old ones now contributing to the unstructured background. Shamma et al. (2011) suggest that this top down influence acts through the principle of temporal coherence. Between the two opposing views, that streams are formed pre-attentively and that multiple streams can co-exist simultaneously, or that attention is required to form a stream and only that single stream is ever present as separated perceptual entity, these findings lend support to the latter.

In summary, these results provide evidence that, in a complex auditory scene with multiple overlapping spectral and temporal sources, the core areas of auditory cortex maintains an acoustic representation of the auditory scene with no significant preference to attended over ignored source, and with no separation into distinct sources. It is only the higher-order auditory areas that provide an object

524 based representation for the foreground, but even there the background remains
525 unsegregated.

526 **References**

527 Ahveninen J, Hamalainen M, Jaaskelainen IP, Ahlfors SP, Huang S, Lin FH, Raij T,
528 Sams M, Vasios CE, Belliveau JW (2011) Attention-driven auditory cortex short-
529 term plasticity helps segregate relevant sounds from noise. Proc Natl Acad Sci U S
530 A 108:4182-4187.

531 Bregman AS (1994) Auditory scene analysis: The perceptual organization of sound: MIT
532 press.

533 Carlyon RP (2004) How the brain separates sounds. Trends Cogn Sci 8:465-471.

534 Chang EF, Rieger JW, Johnson K, Berger MS, Barbaro NM, Knight RT (2010)
535 Categorical speech representation in human superior temporal gyrus. Nat Neurosci
536 13:1428-1432.

537 Cherry EC (1953) Some Experiments on the Recognition of Speech, with One and with 2
538 Ears. Journal of the Acoustical Society of America 25:975-979.

539 Chi T, Ru P, Shamma SA (2005) Multiresolution spectrotemporal analysis of complex
540 sounds. J Acoust Soc Am 118:887-906.

541 David SV, Mesgarani N, Shamma SA (2007) Estimating sparse spectro-temporal
542 receptive fields with natural stimuli. Network 18:191-212.

543 Davis MH, Johnsrude IS (2003) Hierarchical processing in spoken language
544 comprehension. J Neurosci 23:3423-3431.

545 de Cheveigne A, Simon JZ (2007) Denoising based on time-shift PCA. J Neurosci
546 Methods 165:297-305.

547 de Cheveigne A, Simon JZ (2008) Denoising based on spatial filtering. J Neurosci
548 Methods 171:331-339.

549 de Cheveigne A, Parra LC (2014) Joint decorrelation, a versatile tool for multichannel
550 data analysis. Neuroimage 98:487-505.

551 Di Liberto GM, O'Sullivan JA, Lalor EC (2015) Low-Frequency Cortical Entrainment to
552 Speech Reflects Phoneme-Level Processing. Curr Biol 25:2457-2465.

553 Ding N, Simon JZ (2012a) Neural coding of continuous speech in auditory cortex during
554 monaural and dichotic listening. J Neurophysiol 107:78-89.

555 Ding N, Simon JZ (2012b) Emergence of neural encoding of auditory objects while
556 listening to competing speakers. Proc Natl Acad Sci U S A 109:11854-11859.

557 Fritz J, Shamma S, Elhilali M, Klein D (2003) Rapid task-related plasticity of
558 spectrotemporal receptive fields in primary auditory cortex. Nat Neurosci 6:1216-
559 1223.

560 Griffiths TD, Warren JD (2002) The planum temporale as a computational hub. Trends
561 Neurosci 25:348-353.

562 Griffiths TD, Warren JD (2004) What is an auditory object? Nature Reviews
563 Neuroscience 5:887-892.

564 Hickok G, Poeppel D (2007) The cortical organization of speech processing. Nat Rev
565 Neurosci 8:393-402.

566 Inui K, Okamoto H, Miki K, Gunji A, Kakigi R (2006) Serial and parallel processing in
567 the human auditory cortex: a magnetoencephalographic study. Cereb Cortex 16:18-
568 30.

569 Kaas JH, Hackett TA (2000) Subdivisions of auditory cortex and processing streams in
570 primates. Proc Natl Acad Sci U S A 97:11793-11799.

571 Kayser C, Wilson C, Safaai H, Sakata S, Panzeri S (2015) Rhythmic auditory cortex
572 activity at multiple timescales shapes stimulus-response gain and background firing.
573 J Neurosci 35:7750-7762.

574 Kerlin JR, Shahin AJ, Miller LM (2010) Attentional gain control of ongoing cortical
575 speech representations in a "cocktail party". J Neurosci 30:620-628.

576 Lalor EC, Power AJ, Reilly RB, Foxe JJ (2009) Resolving precise temporal processing
577 properties of the auditory system using continuous stimuli. J Neurophysiol 102:349-
578 359.

579 Lutkenhoner B, Mosher JC (2007) Source Analysis of Auditory Evoked Potentials and
580 Fields. In: Auditory evoked potentials : basic principles and clinical application

(Burkard RF, Eggermont JJ, Don M, eds), pp xix, 731 p., 716 p. of plates. Philadelphia: Lippincott Williams & Wilkins.

McDermott JH (2009) The cocktail party problem. Curr Biol 19:R1024-1027.

Mesgarani N, Chang EF (2012) Selective cortical representation of attended speaker in multi-talker speech perception. Nature 485:233-236.

Mesgarani N, David SV, Fritz JB, Shamma SA (2009) Influence of context and behavior on stimulus reconstruction from neural activity in primary auditory cortex. J Neurophysiol 102:3329-3339.

Nelken I, Bar-Yosef O (2008) Neurons and objects: the case of auditory cortex. Front Neurosci 2:107-113.

Ng BS, Schroeder T, Kayser C (2012) A precluding but not ensuring role of entrained low-frequency oscillations for auditory perception. J Neurosci 32:12268-12276.

Nourski KV, Steinschneider M, McMurray B, Kovach CK, Oya H, Kawasaki H, Howard MA, 3rd (2014) Functional organization of human auditory cortex: investigation of response latencies through direct recordings. Neuroimage 101:598-609.

Nourski KV, Reale RA, Oya H, Kawasaki H, Kovach CK, Chen H, Howard MA, 3rd, Brugge JF (2009) Temporal envelope of time-compressed speech represented in the human auditory cortex. J Neurosci 29:15564-15574.

599 O'Sullivan JA, Power AJ, Mesgarani N, Rajaram S, Foxe JJ, Shinn-Cunningham BG,
600 Slaney M, Shamma SA, Lalor EC (2015) Attentional Selection in a Cocktail Party
601 Environment Can Be Decoded from Single-Trial EEG. Cereb Cortex 25:1697-1706.

602 Okada K, Rong F, Venezia J, Matchin W, Hsieh IH, Saberi K, Serences JT, Hickok G
603 (2010) Hierarchical organization of human auditory cortex: evidence from acoustic
604 invariance in the response to intelligible speech. Cereb Cortex 20:2486-2495.

605 Okamoto H, Stracke H, Bermudez P, Pantev C (2011) Sound processing hierarchy within
606 human auditory cortex. Journal of Cognitive Neuroscience 23:1855-1863.

607 Overath T, McDermott JH, Zarate JM, Poeppel D (2015) The cortical analysis of speech-
608 specific temporal structure revealed by responses to sound quilts. Nat Neurosci
609 18:903-911.

610 Pasley BN, David SV, Mesgarani N, Flinker A, Shamma SA, Crone NE, Knight RT,
611 Chang EF (2012) Reconstructing speech from human auditory cortex. PLoS Biol
612 10:e1001251.

613 Peelle JE, Johnsrude IS, Davis MH (2010) Hierarchical processing for speech in human
614 auditory cortex and beyond. Front Hum Neurosci 4:51.

615 Poeppel D, Idsardi WJ, van Wassenhove V (2008) Speech perception at the interface of
616 neurobiology and linguistics. Philos Trans R Soc Lond B Biol Sci 363:1071-1086.

617 Power AJ, Foxe JJ, Forde EJ, Reilly RB, Lalor EC (2012) At what time is the cocktail
618 party? A late locus of selective attention to natural speech. Eur J Neurosci 35:1497-
619 1503.

620 Rauschecker JP, Scott SK (2009) Maps and streams in the auditory cortex: nonhuman
621 primates illuminate human speech processing. Nat Neurosci 12:718-724.

622 Recanzone GH, Guard DC, Phan ML (2000) Frequency and intensity response properties
623 of single neurons in the auditory cortex of the behaving macaque monkey. J
624 Neurophysiol 83:2315-2331.

625 Rouder JN, Speckman PL, Sun D, Morey RD, Iverson G (2009) Bayesian t tests for
626 accepting and rejecting the null hypothesis. Psychon Bull Rev 16:225-237.

627 Särelä J, Valpola H (2005) Denoising source separation. Journal of Machine Learning
628 Research 6:233-272.

629 Schroeder CE, Lakatos P (2009) Low-frequency neuronal oscillations as instruments of
630 sensory selection. Trends Neurosci 32:9-18.

631 Shamma SA, Elhilali M, Micheyl C (2011) Temporal coherence and attention in auditory
632 scene analysis. Trends Neurosci 34:114-123.

633 Shinn-Cunningham BG (2008) Object-based auditory and visual attention. Trends Cogn
634 Sci 12:182-186.

635 Steinschneider M, Liégeois-Chauvel C, Brugge JF (2011) Auditory evoked potentials and
636 their utility in the assessment of complex sound processing. In: The auditory cortex,
637 pp 535-559: Springer.

638 Steinschneider M, Nourski KV, Rhone AE, Kawasaki H, Oya H, Howard MA, 3rd
639 (2014) Differential activation of human core, non-core and auditory-related cortex
640 during speech categorization tasks as revealed by intracranial recordings. Front
641 Neurosci 8:240.

642 Sussman ES, Bregman AS, Wang WJ, Khan FJ (2005) Attentional modulation of
643 electrophysiological activity in auditory cortex for unattended sounds within
644 multistream auditory environments. Cogn Affect Behav Neurosci 5:93-110.

645 Sweet RA, Dorph-Petersen KA, Lewis DA (2005) Mapping auditory core, lateral belt,
646 and parabelt cortices in the human superior temporal gyrus. J Comp Neurol
647 491:270-289.

648 Yuille A, Kersten D (2006) Vision as Bayesian inference: analysis by synthesis? Trends
649 in cognitive sciences 10:301-308.

650 Zion Golumbic E, Cogan GB, Schroeder CE, Poeppel D (2013a) Visual input enhances
651 selective speech envelope tracking in auditory cortex at a "cocktail party". J
652 Neurosci 33:1417-1426.

653 Zion Golumbic EM, Poeppel D, Schroeder CE (2012) Temporal context in speech
654 processing and attentional stream selection: a behavioral and neural perspective.
655 Brain Lang 122:151-161.

656 Zion Golumbic EM, Ding N, Bickel S, Lakatos P, Schevon CA, McKhann GM,
657 Goodman RR, Emerson R, Mehta AD, Simon JZ, Poeppel D, Schroeder CE (2013b)
658 Mechanisms underlying selective neuronal tracking of attended speech at a "cocktail
659 party". Neuron 77:980-991.

660

661 **Legend:**

662 Figure 1: Illustrations of different decoding- and encoding-based neural
663 representations of the auditory scene and its constituents. (*Left)* Examples of
664 predicted MEG neural response using the Early-late model (red) and the
665 Summation model (magenta) superimposed on actual MEG response (black). The
666 proposed Early-late model prediction shows higher correlation with the actual
667 MEG neural response than Summation model. (*Right)* Example of speech
668 envelopes reconstructed (grey) from their late neural responses, for both the
669 foreground and the background, superimposed on actual speech envelopes of
670 foreground (blue) and background (cyan). The foreground reconstruction shows
671 higher correlation with the actual foreground envelope, compared to the
672 background reconstruction with the actual background envelope. All examples are
673 grand averages across subjects (3 seconds duration).

674

675 Figure 2: Early vs. late MEG neural responses to a continuous speech stimulus. A
676 sample stimulus envelope and multi-channel MEG recordings are shown in red
677 and black respectively. The two grey vertical lines indicate two arbitrary time
678 points at t - Δt and t. The dashed and dotted boxes represent the early and late
679 MEG neural responses to stimulus at time point t respectively. The reconstruction

of the stimulus envelope at time *t* can be based on either early or late neural responses, and the separate reconstructions can be compared against each other.

Figure 3: Stimulus envelope reconstruction accuracy using *early* neural responses. **A.** Scatter plot of reconstruction accuracy of the foreground vs. individual background envelopes. No significant difference was observed ($p = 0.21$), and therefore no preferential representation of the foreground speech over the individual background streams is revealed in early neural responses. **B.** Scatter plot of reconstruction accuracy of the envelope of the entire acoustic scene vs. that of the sum of the envelopes of all three individual speech streams. The acoustic scene is reconstructed more accurately (visually, most of data points fall above the diagonal) as a whole than as the sum of individual components in early neural responses ($p < 2 \times 10^{-6}$). Reconstruction accuracy is measured by proportion of the variance explained: the square of the Pearson correlation coefficient between the actual and predicted envelopes.

Figure 4: Stimulus envelope reconstruction accuracy using *late* neural responses. **A.** Scatter plot of accuracy between foreground vs. individual background envelope reconstructions demonstrates that the foreground is represented with

dramatically better fidelity (visually, most of data points fall above the diagonal) than the background speech, in late neural responses ($p < 2 \times 10^{-6}$). **B.** Scatter plot of the reconstruction accuracy of the envelope of the entire background vs. that of the sum of the envelopes of the two individual background speech streams. The background scene is reconstructed more accurately as a monolithic background than as separated individual background streams in late neural responses ($p = 0.012$)

Figure 5: MEG response prediction accuracy. Scatter plot of the accuracy of predicted MEG neural response for the proposed Early-late model vs. the standard Summation model. The Early-late model predicts the MEG neural response dramatically better (visually, most of data points fall above the diagonal) than the Summation model ($p < 2 \times 10^{-6}$). The accuracy of predicted MEG neural responses is measured by proportion of the variance explained: the square of the Pearson correlation coefficient between the actual and predicted responses.

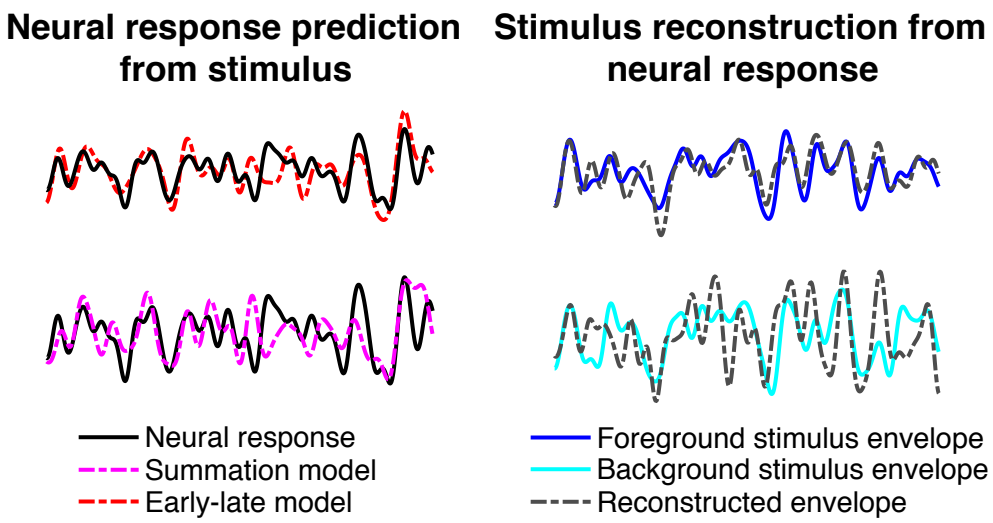

716

717

718 Figure 1

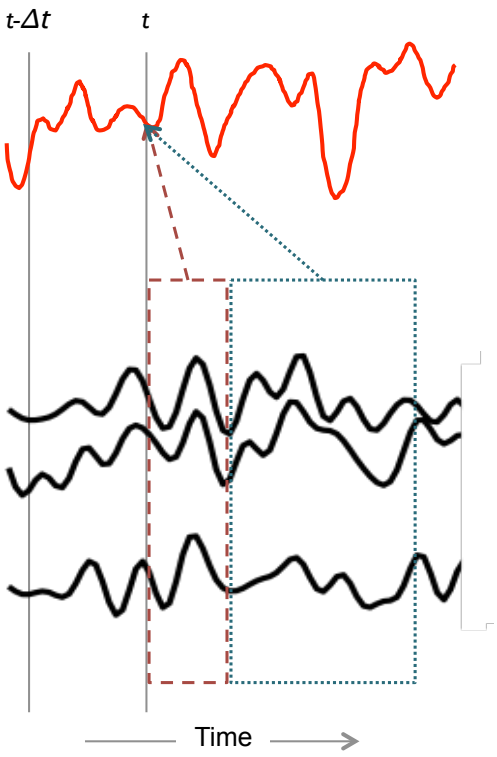

719

720

721 Figure 2

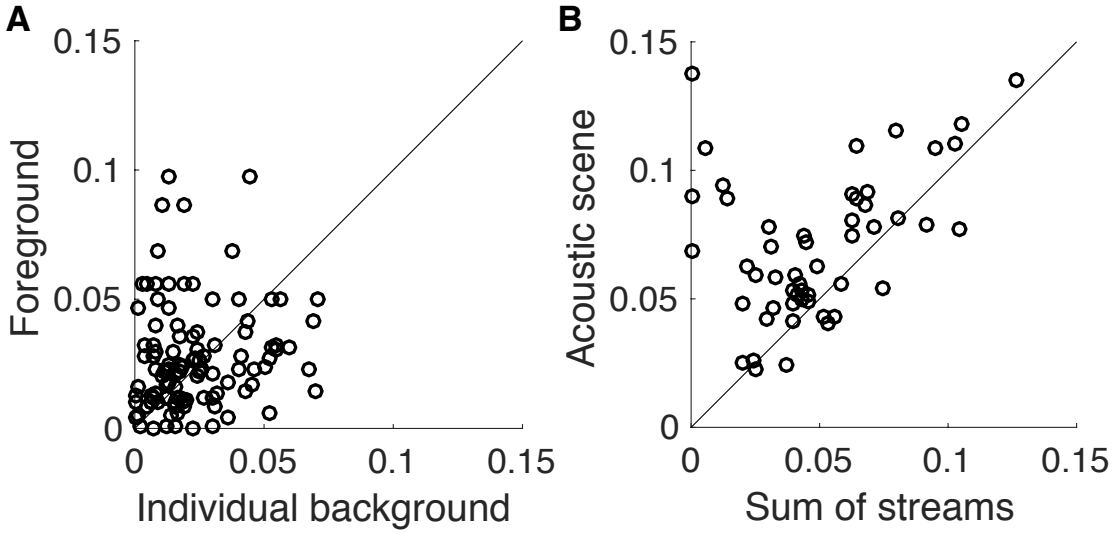

722

723

724 Figure 3

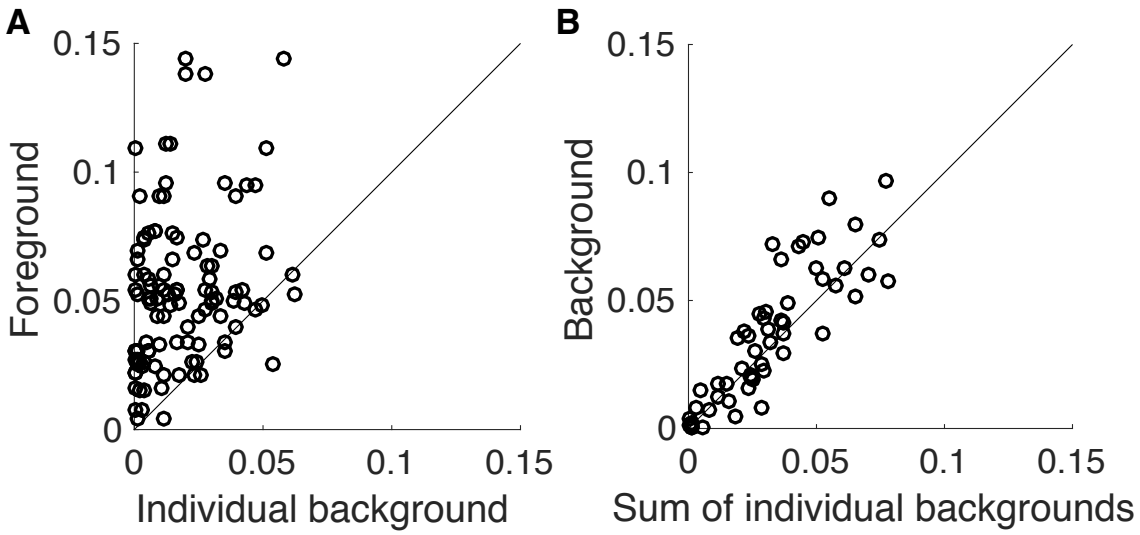

725

726

727 Figure 4

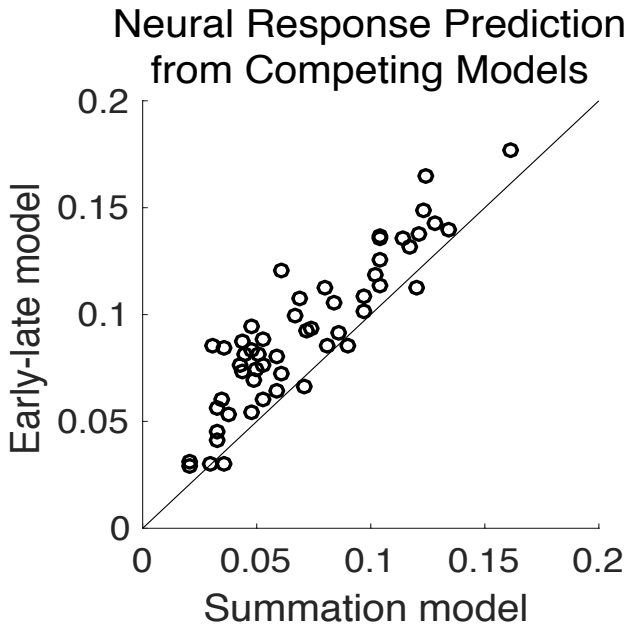

728

729

730 Figure 5